

Micro-XANES: chemical contrast in the scanning transmission X-ray microscope

X. Zhang ^{a,*}, H. Ade ^b, C. Jacobsen ^a, J. Kirz ^a, S. Lindaas ^a, S. Williams ^c, S. Wirick ^a

^a Physics Department, SUNY at Stony Brook, Stony Brook, NY 11794, USA

^b Physics Department, North Carolina State University, Box 8202, Raleigh, NC 27695, USA

^c Biology Department, Brookhaven National Lab, Upton, NY 11973, USA

The scanning transmission X-ray microscope on the X1A undulator beam line, at the National Synchrotron Light Source, has been used for imaging various biological as well as polymer samples at 55 nm Rayleigh resolution. The microscope is operated mainly in direct imaging mode, where X-rays of fixed energy are diffractively focussed to a microprobe and the sample is scanned in two dimensions. However, by varying the X-ray energy while keeping the beam focussed to one spot on the sample we can also determine the localized chemical composition of the sample from the carbon X-ray absorption near edge spectra in an area smaller than 0.2 μm by 0.2 μm . The spatial distribution of the chemical constituents can be obtained by imaging at absorption maxima of specific chemical bonds, while retaining the 0.05 μm spatial resolution of the microscope. The chemical sensitivity of X-ray-absorption near-edge spectroscopy provides a powerful contrast mechanism for imaging organic systems. The well-known differences in energy among π^* resonances of different chemical bonds have been used to distinguish different polymer phases and have been applied to biological systems.

1. Introduction

The scanning transmission X-ray microscope (STXM) is designed to image biological samples in their wet and unstained condition using the high absorption contrast between the organic material and water for photon energies between the carbon and oxygen K absorption edges. It uses the soft X-ray undulator at the National Synchrotron Light Source beam line X1A as its X-ray source. A spherical grating monochromator which is normally operated at a resolving power of 300–900, depending on flux requirements, is used to select an X-ray energy between 250 and 750 eV. The coherent beam is then brought from vacuum to an atmospheric pressure environment through a thin Si_3N_4 window and focussed by a Fresnel zone plate. The sample is scanned in the focal plane and the transmitted flux is detected by a proportional counter and stored digitally in a computer. The spatial resolution of the microscope is limited by the zone plate which has a finest zone width of 45 nm, resulting in a Rayleigh resolution of 55 nm. We have measured the microscope's modulation transfer function (MTF) by imaging a high resolution test pattern using the STXM as well as a scanning transmission electron microscope (STEM) [1,5]. The measured MTFs agree well with the calculations, confirming the performance of the microscope as designed. Fig. 1a shows the

measured and calculated MTFs. Fig. 1b shows the STXM image and the STEM image as well as the deconvolved image of the test pattern using the calculated point spread function. The smallest line in the pattern is 30–35 nm in size.

Besides its imaging mode, where we fix the X-ray energy and scan the sample in the zone plate focal plane to form a two-dimensional image, one can also take a spectrum from a small spot by scanning the monochromator to change the X-ray energy and adjusting the zone plate to sample distance simultaneously to keep the sample in focus at different energies (the zone plate focal length is proportional to the X-ray energy). We have been able to take spectra from an area of 0.2 μm^2 [4]. Combining the imaging mode and the chemical sensitivity of X-ray-absorption near-edge spectroscopy (XANES), here we report some applications to polymer science and biological studies.

2. Polymer science applications of STXM

The ultimate bulk and surface properties of heterophase polymers are strongly tied to their morphology. Light and electron microscopies are often successfully used to characterize such morphologies, but these techniques are inherently limited in their applicability and versatility. With judicious choice of photon energy, XANES microscopy is sensitive to the chemical (unoccupied valence) state and

* Corresponding author.

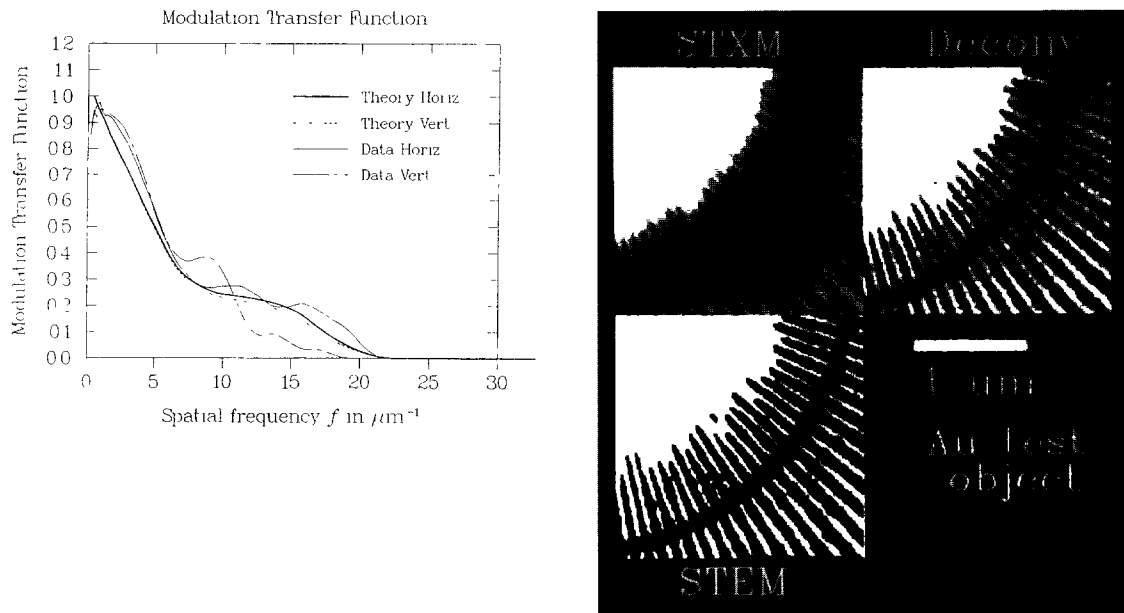


Fig. 1. (a) The calculated and measured MTFs (from ref. [1]). (b) Au test pattern viewed by STXM, STEM and the STXM with deconvolution (from ref. [1]).

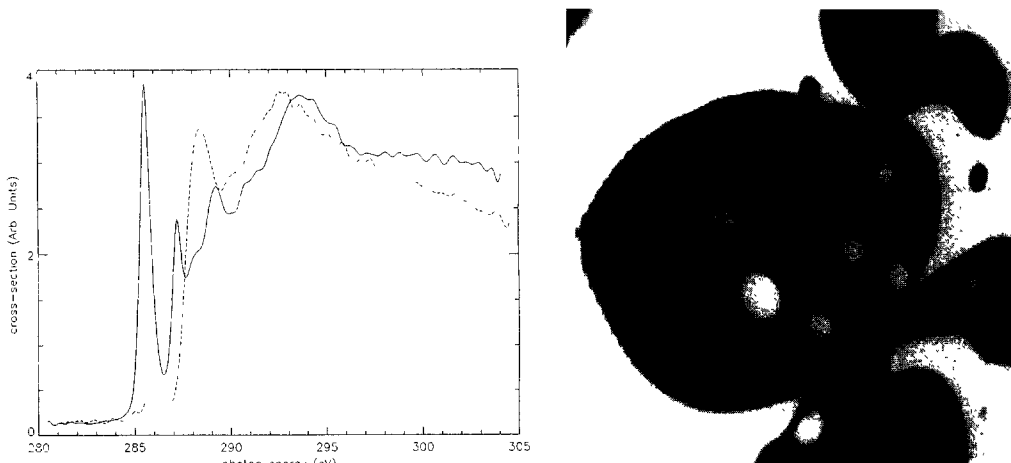


Fig. 2. (a) Carbon XANES spectra of polypropylene (dashed line) and a 50–50 wt% random copolymer of polystyrene and acrylonitrile (solid line) (from ref. [4]). (b) Micrograph of a 0.5 μm -thick section of poly(styrene-acrylonitrile)-polypropylene blend acquired at a photon energy of 285.5 eV. Styrene is strongly absorbing at this energy and the phase containing it appears dark, while polypropylene is virtually transparent. Black and white levels of the micrograph are from zero to incident intensity, i.e. contrast is not enhanced (field of view: 30 $\mu\text{m} \times 30 \mu\text{m}$) (from ref. [4]. Sample courtesy of S. Cameron from EXXON research and engineering).

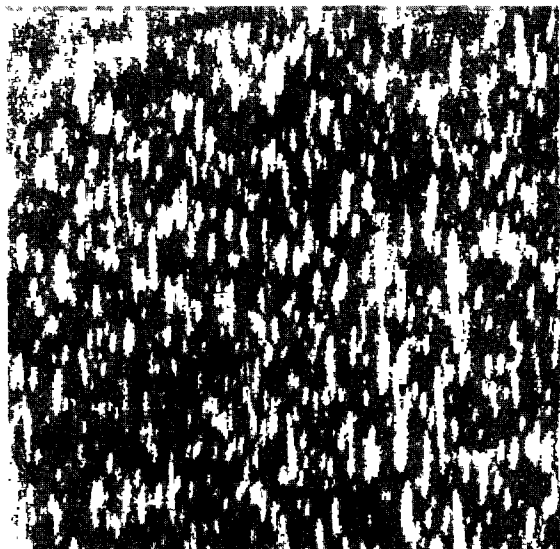


Fig. 3. Micrograph of a PC/PET blend, demonstrating contrast between these homopolymer phases without staining (field of view: $30\ \mu\text{m} \times 30\ \mu\text{m}$). Sample courtesy of G. Mitchell and R. Cieslinsky from Dow Chemical.

local orientation of each component present and is, for instance, capable of distinguishing among chemical functionality such as C–C, C=C, C≡C, C=O, COOH, and C≡N. To demonstrate this chemical sensitivity we imaged several unstained heterophase polymers with very high contrast. In Fig. 2b, a poly(styrene–acrylonitrile)–polypropylene blend was imaged at a photon energy of 285.5 eV. At this energy, styrene is highly absorbing, while the polypropylene matrix is practically transparent [4]. Fig. 2a shows the noticeable differences between the spectra of the two polymers. Fig. 3 shows the chemical contrast of a polycarbonate/poly(ethylene terephthalate) (PC/PET) blend at a photon energy of 285.7 eV. Again, good contrast is achieved without staining.

Besides its chemical sensitivity, XANES is polarization dependent [3] and the resulting X-ray dichroism can be used to image bond orientations in (partially) ordered samples [6,7]. Figs. 4a and 4b are micrographs of a 100-nm-thick section of a poly(*p*-phenylene terephthalamide) (PPTA) fiber imaged with the electric field vector in the left–right direction (a) and up–down direction (b), respectively. Strong contrast changes reflecting orientational sensitivity are readily observable. In these particular images, many of the observed features are sectioning artifacts. They nevertheless demonstrate orientational sensitivity in STXM.

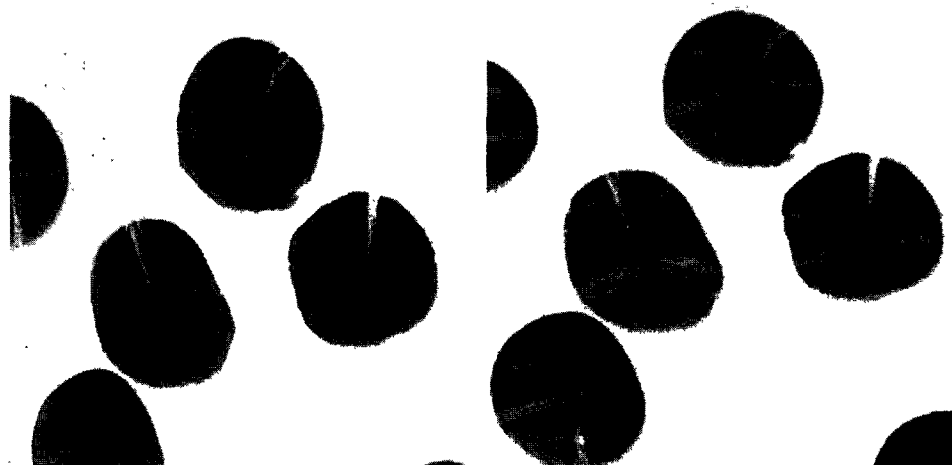


Fig. 4. Micrographs of a $0.1\ \mu\text{m}$ thick PPTA fiber section (cut 45° relative to fiber axis) imaged with electric field vector in left–right direction (a) and in up–down (b) direction at 285.5 eV photon energy. This energy selects the aromatic group of the fiber polymer and contrast changes between these two images arise due to X-ray dichroism reflecting orientational order in the sample. In these particular images weak butterfly-like patterns are caused by the underlying radial symmetry of the fiber, while higher contrast features are due to anisotropies introduced during sectioning (differences in shape of the individual fibers are due to slightly different X–Y magnification (field of view: $40\ \mu\text{m} \times 40\ \mu\text{m}$). Sample courtesy of B. Hsiao and S. Subramoney from DuPont.

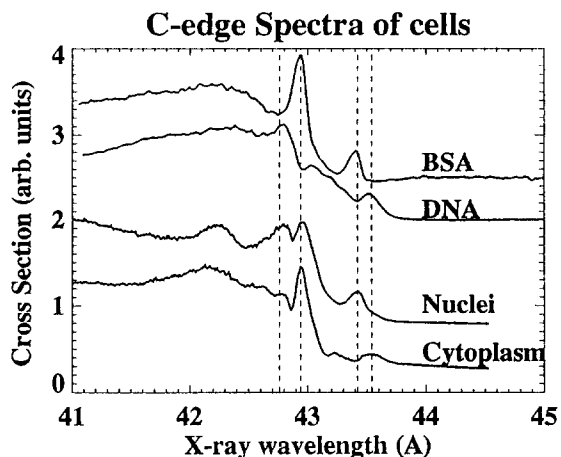


Fig. 5 Top: spectra of DNA and bovine serum albumin (BSA). Due to the different concentration and environment of the bonds in DNA and BSA, the peaks from C=C, C=N, and C=O have different intensities as well as different energies. Bottom: spectra of nucleus and cytoplasm of critical point dried CHO cell. The ratio between the DNA peak (4.275 nm) and BSA peak (4.294 nm) is higher in the spectrum from nucleus than that from cytoplasm, indicating more DNA in nucleus than in cytoplasm.

3. Biological applications

Some biological samples with similar elemental components have different chemical compositions; one should expect differences in their XANES spectra. Proteins and DNA, two important biological components, have different concentrations of C=C, C=N and C=O bonds that give rise to different π^* resonance intensities in XANES [3,4]. The different environment of the same chemical bond in protein and DNA shifts the π^* resonance positions to different energies. The expected difference between the XANES spectra of bovine serum albumin (BSA, a typical protein) and DNA near the carbon absorption edge has been observed with the STXM and is illustrated in Fig. 5 [4]. We have utilized this difference to image chromosomes at different energies corresponding to absorption maxima of protein and DNA to obtain micrographs where the absorption contrast is dominated either by DNA or by protein (Fig. 6). More recently, we have been developing an analytical method to get quantitative mapping of DNA and protein within biological samples through the use of the spectral features from DNA and protein and images of biological samples at wavelengths corresponding to different absorption peaks. Fig. 5 shows the spectra taken from nucleus and cytoplasm of a Chinese hamster ovarian cell.

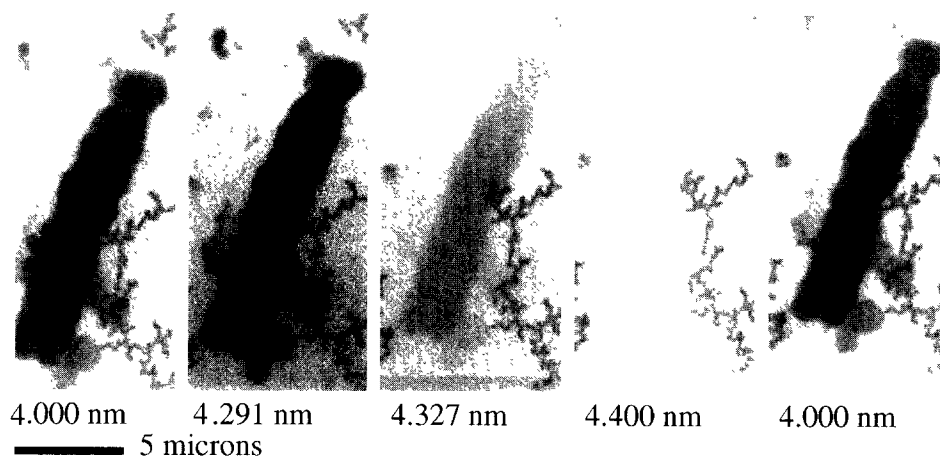


Fig. 6. Images of the same wet, fixed *V. faba* chromosome at different wavelengths corresponding to different absorption maxima as shown in Fig. 5. The high contrast between the chromosome and environment at 4.291 nm is mainly due to the large absorption of protein at this wavelength. Note the image taken at 4.4 nm (which is below the carbon absorption edge) shows no contrast between organic material and water. The last image shows very little difference from the first one, indicating that radiation damage after five images (with a dose from 20 to 50 Mrad in each image) is still tolerable.

The spectrum from the nucleus has a higher DNA (peak at 42.75 Å = 289.6 eV) to protein (peak at 42.94 Å = 288.3 eV) ratio than that from cytoplasm, indicating that there is more DNA in nuclei than in cytoplasm as would be expected. This control study forms a basis for mapping protein and DNA in other specimens.

4. Summary

In the work reported here we have primarily employed the carbon K-edge XANES to acquire images and spectra of polymers and biological samples. However, nitrogen, oxygen, potassium and calcium edges, as well as other core shells with energies in the 250–750 eV range, should be accessible with the X1A microscope. In fact, Buckley et al. utilize the Ca L edge for elemental mapping and are exploring the Ca L XANES differences between various biological Ca salts [8]. For optimum signal-to-noise ratio the samples should be 0.1–0.5 μm in thickness for transmission experiments in the above photon energy range. In principle, it is also possible to make the XANES imaging surface sensitive, selectively probing 1, 10 and 100 nm of the sample surface, by monitoring the near edge cross sections via the Auger-secondary electron-, and fluorescence yield mechanisms, respectively [3,9].

In summary, the chemical sensitivity of the XANES and the high resolution of the X1A STXM allow us to obtain quantitative information on different chemical states and to distinguish systems with similar elemental compositions. These contrast mechanisms, particularly when combined with surface sensitivity, and the low radiation damage of XANES microscopy will make it a valuable charac-

terization tool in a broad range of investigations involving heterogeneous specimens.

Acknowledgments

Part of the polymer work was performed while H. Ade was at SUNY, Stony Brook. This work was supported by NSF grant DIR 9005893. We are grateful to E. Anderson, D. Attwood, and M. Rivers for their support and help with the X-ray microscope. We thank J. Van't Hof and S. Lamm of the Biology Dept. at BNL for their help with the biological sample preparations. We also thank B. Hsiao, and S. Subramoney from DuPont, G. Mitchell and R. Cieslinky from Dow Chemical, and S. Cameron. S. Costello, E. Berluche, J. Chudzinsky, and S. Behal from Exxon Research for providing the polymer samples and for help with the conceptual and actual experiments.

References

- [1] C. Jacobsen et al., *Opt. Commun.* 86 (1991) 351.
- [2] For recent applications, see *Soft X-ray Microscopy*, eds. C. Jacobsen and J. Trebes, *SPIE Proc.* 1741 (1992).
- [3] J. Stöhr, *NEXAFS Spectroscopy*, Springer Series in Surface Science, vol. 25 (Springer, Berlin, 1992).
- [4] H. Ade et al., *Science* 258 (1992) 972.
- [5] X. Zhang et al., *SPIE* 1741 (1992) 251.
- [6] H. Ade, B. Hsiao, G. Mitchell, S. Cameron and S. Costello. *MSA Proc.* (1993).
- [7] H. Ade and B. Hsiao *Science* 262 (1993) 1427.
- [8] C.J. Buckley et al., *Rev. Sci. Instr.* 63 (1992) 588.
- [9] G.R. Harp, Z.L. Han and B.P. Tonner, *J. Vac. Sci. Technol. A* 8 (1990) 2566.